Acta Acustica 2024, **8**, 26

https://doi.org/10.1051/aacus/2024022

Special Issue: Numerical, computational and theoretical acoustics

Available online at:
https://acta-acustica.edpsciences.org

SCIENTIFIC ARTICLE OPEN ACCESS

A localized approximation approach for the calculation of beam shape coefficients of acoustic and ultrasonic Bessel beams

Leonardo A. Ambrosio[1,*] and Gérard Gouesbet[2]

[1] Department of Electrical and Computer Engineering, São Carlos School of Engineering, University of São Paulo, 400 Trabalhador são-carlense Ave. 13566-590, São Carlos, SP, Brazil
[2] CORIA-UMR 6614 – Normandie Université, CNRS-Université et INSA de Rouen, Campus Universitaire du Madrillet, 76800 Saint-Etienne du Rouvray, France

Received 31 December 2023, Accepted 5 June 2024

Abstract – The description of acoustical waves can be achieved using an expansion over basic functions with weighting coefficients which may be called beam shape coefficients (BSCs). There is a strong analogy between the scalar formalism of acoustical waves and the vectorial electromagnetic formalism, known as generalized Lorenz–Mie theory (GLMT), describing the interaction between a homogeneous sphere and an arbitrary illuminating beam. In particular, BSCs have been introduced as well in GLMT and the mathematical arsenal to evaluate them, developed since several decades, can be used mutatis mutandis to evaluate BSCs in acoustics. In particular, the present paper introduces a method named localized approximation to the evaluation of the acoustical BSCs, similar to the localized approximation used to evaluate electromagnetic BSCs, in the case of Bessel beams. Such a formalism akin to the electromagnetic GLMT may be viewed as an acoustical GLMT and should allow a renewal of the calculation of various properties of acoustical wave scattering, in particular to the design of acoustical tweezers similar to optical tweezers.

Keywords: Acoustic scattering, Beam shape coefficients, Bessel beams, Generalized Lorenz–Mie theory, Localized approximation

1 Introduction

In some laser light scattering theories, like in generalized Lorenz–Mie theories (GLMTs), e.g. [1, 2], or in Extended Boundary Condition Method (EBCM) for structured beams, e.g. [3–5], the illuminating laser beam may be encoded using beam shape coefficients (BSCs) which intervene when expanding the fields over vector wave functions. There exists an arsenal to evaluate these BSCs, including quadratures and localized approximations (LAs), e.g. Gouesbet et al. for a review [6].

It however happens that the structure of scalar scattering theories exhibits many analogies with the one of vectorial scattering discussed above, so that the arsenal developed in this framework, may be transferred, *mutatis mutandis*, to the case of acoustical scattering. The present paper is then devoted to a discussion of quadratures and localized approximation methods to the case of acoustical Bessel beams.

When no analytical, rigorous solutions can be found for the BSCs, it is usually advantageous to have recourse to alternative, approximate schemes such as the LAs [7–9]. Although widely known and explored in optics, these methods remained largely overlooked in the field of acoustic scattering.

To the best of the authors' knowledge, the first paper that introduced the concept of localized approximations for explicit BSC calculation in acoustic scattering appeared in 2022 and is due to Li et al. in the evaluation of radiation forces on elastic spheres [10]. In this work, LA BSCs are calculated for Gaussian-like beams under both on- and off-axis configurations, the BSCs for the latter configuration being found from the former through the use of a translational addition theorem of spherical wave functions. Then, in 2023, Li and Zhang, again using LA schemes, evaluated acoustic forces over multilayered, eukaryotic spherical cells arbitrarily positioned in space with respect to a Gaussian beam [11]. In both works, LA schemes as borrowed from optics were shown to provide good results, with the proviso that the confinement parameter remains small. Finally, and also in the field of scattering by acoustic beams, the van de Hulst principle of localization has been introduced by Marston in 2007 in the interpretation of the scattering dependence on the axicon angle of Bessel beams [12] and in the analysis of scattering of focused beams by spheres considering quasi-Gaussian Bessel beam superpositions [13].

*Corresponding author: leo@sc.usp.br

The paper is organized as follows. Section 2 deals with generalities for arbitrary shaped acoustical waves satisfying the Helmholtz equation, and introduces acoustical BSCs using a quadrature approach. Section 3 deals with the LA-procedure using an empirical approach, introduces a variant named Integral Localized Approximation (ILA), and applies it to the case of on- and off-axis Bessel beams. Section 4 provides simulation results and discussions, which validate the localization procedures for beams having small axicon angles and in the absence of topological charges.

These observations are similar to the ones obtained in optics where it has been observed that the quality of the procedures deteriorates when the axicon angle increases [14–19], and/or when the topological charge increases [20–23]. These observations concerning the LAs reinforce the parallel between vectorial and scalar scatterings. Section 5 is a conclusion.

2 Generalities

Let us start by introducing the usual set of two Cartesian coordinate systems (x, y, z) and (u, v, w) in acoustic and ultrasonic scattering, with origins at O_P and O_B, respectively, see Figure 1. The first system is assumed to be attached to a homogeneous spherical particle and the second to the incident beam. Here, $+u$, $+v$ and $+w$ are parallel to $+x$, $+y$ and $+z$, respectively. Even though we shall not be interested in the geometrical and physical properties of the scatterer, the relative position (x_0, y_0, z_0) of the beam with respect to the center of the sphere (at which the origin O_P is located) is of importance. For $x_0 = y_0 = 0$ and $\pm z$ propagation, we have the simplified on-axis configuration, while for arbitrary $x_0, y_0 \neq 0$, the beam is under an off-axis configuration. Spherical (r, θ, ϕ) and cylindrical (ρ, ϕ, z) coordinates are attached to (x, y, z) for convenience and further calculations. In cylindrical coordinates, the relative position of O_B is designated as (ρ_0, ϕ_0, z_0).

Let us assume a $+z$-propagating incident acoustical beam with a time harmonic factor $\exp(+i\omega t)$, where ω is the operating frequency, written in terms of a complex scalar potential $\psi_i(r, \theta, \phi)$ expressed as a partial wave expansion using spherical wave functions [24–26]:

$$\psi_i(r, \theta, \phi) = \psi_i^0 \sum_{n=0}^{\infty} \sum_{m=-n}^{n} c_n^{pw} g_n^m j_n(kr) P_n^{|m|}(\cos\theta) e^{im\phi}, \quad (1)$$

where ψ_i^0 is the field strength, $c_n^{pw} = (-i)^n(2n+1)$ ("pw" stands for "plane wave"), $j_n(.)$ are spherical Bessel functions of the first kind and of integer order n and $P_n^m(\cos\theta)$ are associated Legendre functions, which follows Robin's convention [27]. This choice for $P_n^m(\cos\theta)$ reflects the preference of the authors and incorporate a factor of $(-1)^m$ which might not be present in other works. Finally, $k = 2\pi/\lambda$ is the wave number and λ is the wavelength. Assuming the absence of nonlinear effects and propagation of the acoustical waves in a lossless medium [28–32], equation (1) is a rigorous solution to the scalar Helmholtz equation which can be used to describe acoustic radiation pressure fields in inviscid fluids.

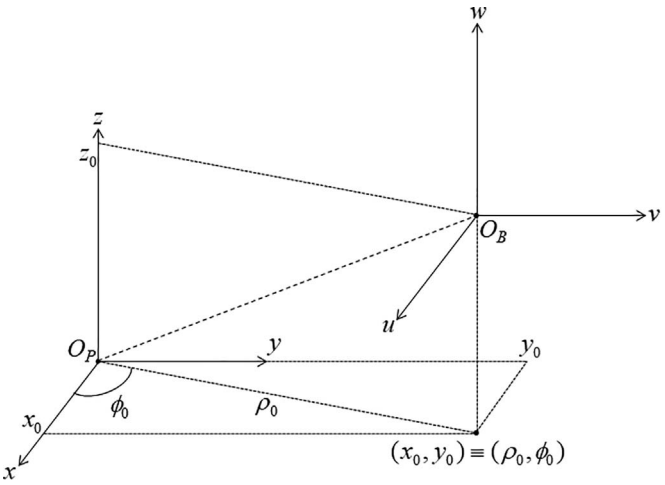

Figure 1. Coordinate systems for acoustic-matter analysis. A Cartesian coordinate system (x, y, z) is introduced supposing a hypothetical spherical scatterer centered at its origin O_P. A second Cartesian coordinate system (u, v, w) is attached to the impinging beam, with origin O_B. The position of O_B with respect to O_P is here denoted as (x_0, y_0, z_0). Attached to the xyz system is a cylindrical coordinate system (ρ, ϕ, z) such that the relative position of O_B can also be written as (ρ_0, ϕ_0, z_0).

The expansion coefficients g_n^m – known as the Beam Shape Coefficients (BSCs) – can be isolated in equation (1) using orthogonality relations for $P_n^m(\cos\theta)$ and $\exp(im\phi)$, see e.g. Refs. [2, 24, 33]:

$$g_n^m = \frac{1}{4\pi c_n^{pw}} \frac{(n-|m|)!}{(n+|m|)!} \frac{2n+1}{j_n(kr)} \times \int_0^{2\pi} \int_0^{\pi} \frac{\psi_i(r, \theta, \phi)}{\psi_i^0} P_n^{|m|}(\cos\theta) e^{-im\phi} \sin\theta \mathrm{d}\theta \mathrm{d}\phi. \quad (2)$$

For beams which exactly satisfy the scalar Helmholtz equation $\nabla^2\psi_i + k^2\psi_i = 0$, the r-dependent factor $1/j_n(kr)$ is cancelled after integration. This is the case of Bessel beams, see Gong et al. [34]. The BSCs calculated from equation (2) are called the *quadrature* BSCs.

3 The localized approximation

According to the localization principle of van de Hulst [35], one can associate to each partial wave in equation (1) (or to each term of order n in the plane wave amplitude functions [2]) an acoustical ray or bundle of rays parallel to the w axis and travelling at a transverse distance $(n+1/2)/k$ from O_{uvw}. The formal justification for the use of a LA approach in optics relies on the asymptotic behavior of Bessel functions of order $(n+1/2)$ in the expressions for the Mie scattering coefficients [2, 35]. Since similar functions also appear for spherical scatterers in acoustics, see equation (5) in Mitri and Silva [36] for the case of a rigid sphere, Mitri [37] (Appendix B) for the general case of an elastic sphere in an ideal fluid and equation (4) in Hasegawa [38] for both fluid and solid isotropic

spheres, it is plausible to conjecture that a LA scheme do indeed exist in acoustics.

Let $R = kr$. Slightly modifying a procedure justified in optics [39], we then empirically propose the following procedure for finding the acoustic LA BSCs as follows:

(i) Decompose the original, intended field ψ_i into azimuthal waves:

$$\psi_i = \sum_m \psi_i^m. \tag{3}$$

(ii) Express the azimuthal modes ψ_i^m under a form that emphasizes a "plane wave" factor which is multiplied by the remaining part of ψ_i^m, viz., $\overline{\psi_i^m}$:

$$\psi_i^m = \left\{A_i^0 e^{-\mathrm{i}R\cos\theta} e^{\mathrm{i}m\phi}\right\}\overline{\psi_i^m}, \tag{4}$$

where A_i^0 is the field strength [e.g., ψ_i^0 of equation (1)].

(iii) Then, the localized approximation $g_{n,LA}^m$ to g_n^m is given by:

$$g_{n,LA}^m = \left(\frac{-\mathrm{i}}{L^{1/2}}\right)^{|m|} \overline{\psi_i^m}\left(R = L^{1/2}, \theta = \pi/2\right), \tag{5}$$

where $L \equiv L(n)$ is a function of n and is still to be found, see below.

It is seen from equations (3)–(5) that the azimuthal waves ψ_i^m carry a plane wave factor $\psi_i^0 \exp(-\mathrm{i}R\cos\theta)$ which, together with the ϕ-dependent exponential $\exp(\mathrm{i}m\phi)$, is removed before application of a localization operator, say $\widehat{G}[.]$, which sets $\theta \to \pi/2$ and $R = kr \to L^{1/2}$. In compact form, therefore, the LA BSCs can be written as:

$$g_{n,LA}^m = Z_n^m \widehat{G}\left[\overline{\psi_i^m}\right], \tag{6}$$

with

$$Z_n^m = \left(\frac{-\mathrm{i}}{L^{1/2}}\right)^{|m|}. \tag{7}$$

For a plane wave of the form $\psi_i = \psi_i^0 \exp(-\mathrm{i}kz) = \psi_i^0 \exp(-\mathrm{i}R\cos\theta)$, one sees that $\overline{\psi_i^m} = \delta_{m,0}$, where δ_{ij} is the Kronecker delta. Therefore, $g_{n,LA}^m = g_n^m = \delta_{m,0}$, $\forall n$, as expected [40, 41].

An important point concerns the choice of L in the LA scheme and, consequently, of Z_n^m. In Refs. [10, 11], no explicit mention to a choice of L is made, since for on-axis Gaussian beams, the only non-zero LA BSCs are those for which $m = 0$ and, therefore, $Z_n^m = 1$ regardless of the choice of L, see equation (5) of Li et al. [10]. For off-axis beams, the use of addition theorem for evaluating g_n^m obscures the explicit appearance of Z_n^m, so that a general formalism cannot be devised from such an approach.

But in the optical domain, Z_n^m have different expressions for $m = 0$ and $m \neq 0$ [9, 42], and it could be the case that $L^{1/2}$ should assume different values for different m as well. That such is not the case is inspired by the rigorous procedure presented by Gouesbet [39] in optics and, after an empirical slight modification, we propose:

$$Z_n^m = \left(\frac{-\mathrm{i}}{n+1/2}\right)^{|m|}, \tag{8}$$

valid for both on- and off-axis beams. In other words, since now $L^{1/2} = n + 1/2$, the $\widehat{G}$ operator will set $\theta \to \pi/2$ and $R = kr \to n + 1/2$.

The quality of the empirical procedure is now checked by modeling the case of Bessel beams.

3.1 LA BSCs for acoustical Bessel beams

An acoustic or ultrasonic Bessel beam is an ideal solution to the scalar homogeneous Helmholtz equation in cylindrical coordinates. It carries resistance to diffraction and, consequently, self-healing properties, so that their transverse field profile is, except for phase variations, invariant under propagation [43, 44].

Let a v-order Bessel beam with axicon angle α have transverse and radial wave numbers $k_\rho = k\sin\alpha$ and $k_z = k\cos\alpha$, respectively. For on-axis beams ($x_0 = y_0 = 0$) with $z_0 = 0$, we can express it as:

$$\psi_i(\rho, \phi, z) = \psi_i^0 J_v(k_\rho \rho) e^{\mathrm{i}v\phi} e^{-\mathrm{i}k_z z}. \tag{9}$$

For off-axis beams, the field of equation (9) is displaced by (x_0, y_0, z_0). Instead of equation (9), one then finds an expression in terms of cylindrical coordinates ρ, ϕ and z:

$$\psi_i(\rho, \phi, z) = \psi_i^0 J_v(k_\rho \rho_G) e^{\mathrm{i}v\phi_G} e^{-\mathrm{i}k_z(z-z_0)}, \tag{10}$$

where

$$\begin{aligned}
\rho_G &= \left[\rho^2 + \rho_0^2 - 2\rho\rho_0\cos(\phi - \phi_0)\right]^{1/2},\\
\rho_0 &= \sqrt{x_0^2 + y_0^2},\\
\phi_0 &= \tan^{-1}\frac{y_0}{x_0},\\
\phi_G &= \tan^{-1}\left(\frac{y - y_0}{x - x_0}\right).
\end{aligned} \tag{11}$$

In order to expand equation (10) into azimuthal modes, we proceed as follows. First, we introduce Neumann's addition theorem for Bessel functions [45]:

$$J_v(k_\rho\rho_G) e^{\mathrm{i}v\phi_G} = \sum_{p=-\infty}^{\infty} J_p(Z_0) J_{p+v}(Z) e^{-\mathrm{i}p\phi_0} e^{\mathrm{i}(v+p)\phi}, \tag{12}$$

with

$$\begin{aligned}
Z_0 &= k_\rho\rho_0,\\
Z &= k_\rho\rho.
\end{aligned} \tag{13}$$

From equations (12) and (13), equation (10) can be rewritten as:

$$\psi_i(\rho, \phi, z) = \psi_i^0 \sum_{p=-\infty}^{\infty} J_p(Z_0) J_{p+v}(Z) e^{\mathrm{i}(v+p)\phi} e^{-\mathrm{i}k_z z} e^{-\mathrm{i}p\phi_0} e^{\mathrm{i}k_z z_0}. \tag{14}$$

Now, let $m = p + v$, or $p = m - v$. Then, from equation (14),

$$\psi_i(\rho,\phi,z) = \sum_{m=-\infty}^{\infty} \left[\psi_i^0 J_{m-v}(Z_0) J_m(k_\rho \rho) e^{-\mathrm{i}(m-v)\phi_0} e^{\mathrm{i}k_z z_0}\right] e^{\mathrm{i}m\phi} e^{-\mathrm{i}k_z z}, \tag{15}$$

which, for highly paraxial beams, $\cos\alpha \approx 1$, and $\exp(-\mathrm{i}k_z z) = \exp(-\mathrm{i}k\cos\alpha z) \approx \exp(-\mathrm{i}kz) = \exp(-\mathrm{i}kr\cos\theta)$. This means that, under this restrict case, a plane wave factor of the form $\psi_i^0 \exp(-\mathrm{i}k\cos\theta)$ can be put into evidence in equation (15). Using the fact that $R = kr$, equation (15) can then be recast under the form:

$$\psi_i(\rho,\phi,z) \approx \sum_{m=-\infty}^{\infty} \left\{\psi_i^0 e^{-\mathrm{i}R\cos\theta} e^{\mathrm{i}m\phi}\right\} \left[J_{m-v}(Z_0) J_m(k_\rho\rho) e^{-\mathrm{i}(m-v)\phi_0} e^{\mathrm{i}k_z z_0}\right]. \tag{16}$$

Notice that the condition of highly paraxial beams is necessary to ensure a quasi-plane wave factor under the brackets of equation (16), but that we have not applied the paraxial approximation $\cos\alpha \approx 1$ and $\sin\alpha \approx \alpha$ to the remaining part of equation (15) because, for all practical purposes regarding the determination of an approximate expression for the BSCs, the paraxial approximation does not need to be forced to hold for all factors in equation (16). As observed in optics using a variant known as the *integral* localized approximation, the LA is not able to accurately remodel a Bessel beam for high axicon angles [16].

Comparison between equations (4) and (16) allows us to identify $\overline{\psi_i^m}$. Using the fact that $k\rho = kr\sin\theta$, one then finds:

$$\overline{\psi_i^m} = J_{m-v}(Z_0) J_m(R\,\sin\,\alpha\,\sin\,\theta) e^{-\mathrm{i}(m-v)\phi_0} e^{\mathrm{i}k\cos\alpha z_0}. \tag{17}$$

Applying the localization operator $\widehat{G}[.]$ on equation (17) leads to

$$\widehat{G}\left[\overline{\psi_i^m}\right] = J_{m-v}(Z_0) J_m\left[\left(n+\frac{1}{2}\right)\sin\alpha\right] e^{-\mathrm{i}(m-v)\phi_0} e^{\mathrm{i}k\cos\alpha z_0}. \tag{18}$$

Substituting equation (18) in equation (6) and making use of equation (8) then leads to the final expression for the BSCs of a general off-axis arbitrary-order Bessel beam:

$$g_{n,LA}^m = \left(\frac{-\mathrm{i}}{n+1/2}\right)^{|m|} J_{m-v}(Z_0) J_m\left[\left(n+\frac{1}{2}\right)\sin\alpha\right] e^{-\mathrm{i}(m-v)\phi_0} e^{\mathrm{i}k_z z_0}, \tag{19}$$

with Z_0 given by equation (13).

Equation (19) is the most important formula of the present work. It can be readily compared with the exact BSCs calculated from quadratures [34] which, using the time harmonic convention $\exp(+\mathrm{i}\omega t)$, can be recast under the form:

$$g_{n,exa}^m = (-1)^m \mathrm{i}^{-|m|} \frac{(n-m)!}{(n+|m|)!} J_{m-v}(Z_0) P_n^m(\cos\alpha) e^{-\mathrm{i}(m-v)\phi_0} e^{\mathrm{i}k_z z_0}. \tag{20}$$

Since $(-1)^m = (-1)^{|m|}$ and $\mathrm{i}^{-|m|} = (-\mathrm{i})^{|m|}$, $g_{n,exa}^m$ can be put in a form best suited for comparison with $g_{n,LA}^m$:

$$g_{n,exa}^m = (-1)^{|m|}(-\mathrm{i})^{|m|} \frac{(n-m)!}{(n+|m|)!} J_{m-v}(Z_0) P_n^m(\cos\alpha) e^{-\mathrm{i}(m-v)\phi_0} e^{\mathrm{i}k_z z_0}. \tag{21}$$

For on-axis beams ($Z_0 = 0$), equations (19) and (21) simplify, respectively, to:

$$g_{n,LA}^m = \left(\frac{-\mathrm{i}}{n+1/2}\right)^{|m|} J_m\left[\left(n+\frac{1}{2}\right)\sin\alpha\right] e^{\mathrm{i}k_z z_0} \delta_{m,v} \tag{22}$$

and

$$g_{n,exa}^m = (-1)^{|m|}(-\mathrm{i})^{|m|} \frac{(n-m)!}{(n+|m|)!} P_n^m(\cos\alpha) e^{\mathrm{i}k_z z_0} \delta_{m,v}. \tag{23}$$

It is seen that, for on-axis Bessel beams, the only non-zero BSCs are those with $m = v$, as expected [34].

3.2 Asymptotic correspondence between the LA and exact BSCs

Besides the N-beam method used in optics, and under study in acoustics, an alternative way to at least partially justify the choice of Z_n^m for acoustical fields is by looking at the asymptotic behavior of the associated Legendre polynomials for large n ($n \to \infty$) and small axicon angles.

To see it clearly, let [33]

$$P_n^m(\cos\alpha) = \frac{(n+m)!}{(n-m)!}(-1)^m P_n^{-m}(\cos\alpha), \tag{24}$$

so that, from equation (21), $g_{n,exa}^m$ for $m \geq 0$ can be put under the form

$$g_{n,exa}^{m\geq 0} = \mathcal{G}(-\mathrm{i})^m P_n^{-m}(\cos\alpha), \tag{25}$$

where

$$\mathcal{G} = J_{m-v}(Z_0) e^{-\mathrm{i}(m-v)\phi_0} e^{\mathrm{i}k_z z_0}. \tag{26}$$

Similarly, for $m < 0$, it is readily seen from equations (21) and (26) that

$$g_{n,exa}^{m<0} = \mathcal{G}(-\mathrm{i})^{|m|}(-1)^{|m|} P_n^{-|m|}(\cos\alpha). \tag{27}$$

In a similar fashion, from equation (19), it is inferred that:

$$g_{n,LA}^{m\geq 0} = \mathcal{G}\left(\frac{-\mathrm{i}}{n+1/2}\right)^m J_m\left[\left(n+\frac{1}{2}\right)\sin\alpha\right] \tag{28}$$

and, remembering that $J_{-m}(x) = (-1)^m J_m(x)$,

$$g_{n,LA}^{m<0} = \mathcal{G}\left(\frac{-\mathrm{i}}{n+1/2}\right)^{|m|} (-1)^{|m|} J_{|m|}\left[\left(n+\frac{1}{2}\right)\sin\alpha\right]. \tag{29}$$

Next, we introduce the MacDonald expansion for associated Legendre polynomials as their degree $n \to \infty$, see equation (1), Section 5.72 in Watson [45]:

$$P_n^{-|m|}(\cos\alpha) = \left(n+\frac{1}{2}\right)^{-|m|}\left(\cos\frac{\alpha}{2}\right)^{-|m|}\left[J_{|m|}(x) + \sin^2\frac{\alpha}{2}\left\{\frac{1}{6}xJ_{|m|+3}(x) - J_{|m|+2} + \frac{1}{2}x^{-1}J_{|m|+1(x)}\right\} + \ldots\right], \tag{30}$$

with $x = 2(n+1/2)\sin(\alpha/2)$.

For highly paraxial beams, a first approximation can be set with $\cos\alpha/2 \approx 1$ and $\sin(\alpha/2) \approx \alpha/2$, such that $x \approx (n+1/2)\alpha \approx (n+1/2)\sin\alpha$ and, retaining only the first term in equation (30),

$$P_n^{-|m|} \approx \left(n+\frac{1}{2}\right)^{-|m|} J_{|m|}\left[\left(n+\frac{1}{2}\right)\sin\alpha\right], \quad n \to \infty,\ \alpha\,(\text{very})\,\text{small}. \tag{31}$$

It is then seen from equations (25), (27)–(29) and (31) that, for sufficiently small axicon angles, large n and for all m, $g^m_{n,exa}/g^m_{n,LA} \to 1$. Under these conditions, the choice $R = L^{1/2} = (n+1/2)$ is fully appropriate. Since $L^{1/2}$ must be independent of the choice of the acoustical field (otherwise, one would have to deal with a different LA scheme for each incident beam, therefore leading to an infinite number of LAs), it is admissible at the present time to take this form of $L^{1/2}$ to be best suited for achieving accurate results using the LA approach.

3.3 The acoustical *integral* localized approximation

In 1998, Ren et al. proposed a variation of the LA scheme whose main advantage was to avoid, in the process of obtaining the BSCs of optical wave fields, the decomposition into azimuthal modes, which corresponds in the acoustical or ultrasonic case to equation (3) above.

The main idea behind such proposal was to gain a certain level of flexibility in dealing with arbitrary-shaped beams, since such a decomposition could, in principle, be tedious.

Such an approach can be readily translated to acoustic and ultrasonic fields. Since the modes ψ_i^m in equation (3) are proportional to $\exp(im\phi)$ [for Bessel beams, this is seen from equation (15)] and using simple orthogonality relations for exponential functions, step (i) in the LA scheme can be avoided if we evaluate ψ_i^m according to:

$$\psi_i^m = \frac{1}{2\pi}e^{im\phi}\int_0^{2\pi}\psi_i(r,\theta,\phi')e^{-im\phi'}\mathrm{d}\phi'. \tag{32}$$

In view of equations (6) and (32), the BSCs can now be found from:

$$g_n^m = \frac{Z_n^m}{2\pi}\int_0^{2\pi}\frac{\widehat{G}[\psi_i(r,\theta,\phi)]}{\psi_i^0}e^{-im\phi}\mathrm{d}\phi. \tag{33}$$

Because equation (33) now involves an integration process, this new LA scheme has been given the name *integral* localized approximation (ILA) [9].

The fact is that, for off-axis Bessel beams, the extraction of the BSCs from equation (33) still demands the expansion of $\psi_i(r,\theta,\phi)$ into azimuthal modes before performing the ϕ-integration. This has been shown to hold for both zero-order and higher-order optical Bessel beams, where azimuthal modes appears naturally when using Neumann's addition theorem for Bessel functions [42, 46].

Starting from equation (10), imposing the localization operator $\widehat{G}[.]$, expanding the resulting formula according to Neumann's addition theorem and performing the integration over ϕ, the BSCs extracted from equation (33) using the ILA can be shown to be the same as those derived from the LA itself and given in equation (19), as expected.

3.4 A general relation between exact and LA BSCs

An interesting and general relation between the exact and LA BSCs for acoustic/ultrasonic fields can be extracted from equations (1) and (33).

To see it clearly, notice that the localization operator, once applied on equation (1), produces

$$\widehat{G}[\psi_i(r,\theta,\phi)] = \psi_i^0\sum_{p=0}^{\infty}\sum_{q=-p}^{p}c_p^{pw}g_{p,exa}^q j_p\left(p+\frac{1}{2}\right)P_p^{|q|}(0)e^{iq\phi}, \tag{34}$$

where we have explicitly written the r.h.s. in terms of the exact BSCs.

Now, from equation (33),

$$g^m_{n,LA} = \frac{Z_n^m}{2\pi}\int_0^{2\pi}\sum_{p=0}^{\infty}\sum_{q=-p}^{p}c_p^{pw}g_{p,exa}^q j_p\left(n+\frac{1}{2}\right)P_p^{|q|}(0)e^{i(q-m)\phi}\mathrm{d}\phi = Z_n^m\sum_{p=0}^{\infty}c_p^{pw}g^m_{p,exa}j_p\left(n+\frac{1}{2}\right)P_p^{|m|}(0). \tag{35}$$

Equation (35) establishes an intrinsic relation between $g^m_{n,LA}$ and the exact BSCs of arbitrary-shaped beams. Since [27]

$$P_p^{|m|}(0) = \begin{cases}(-1)^{\frac{p+|m|}{2}}\dfrac{(p+|m|-1)!!}{2^{\frac{p-|m|}{2}}\left(\frac{p-|m|}{2}\right)!}, & (p-|m|)\text{even}\\ 0, & \text{otherwise},\end{cases} \tag{36}$$

where (.)!! is the double factorial, in general only a set of exact BSCs [either with $(p-m)$ even or $(p-m)$ odd] will contribute to the value of $g^m_{n,LA}$. In addition, because $P_p^{|m|}(0) = 0$ for $p < |m|$, equation (35) can be written in the following final form:

$$g^m_{n,LA} = Z_n^m\sum_{p=|m|}^{\infty}c_p^{pw}g^m_{p,exa}j_p\left(n+\tfrac{1}{2}\right)P_p^{|m|}(0). \tag{37}$$

The importance of equation (37) relies on the fact that, whenever a comparison between exact and LA BSCs is to be performed, or when one needs to infer the limit of applicability of the LA for a particular beam whose exact BSCs

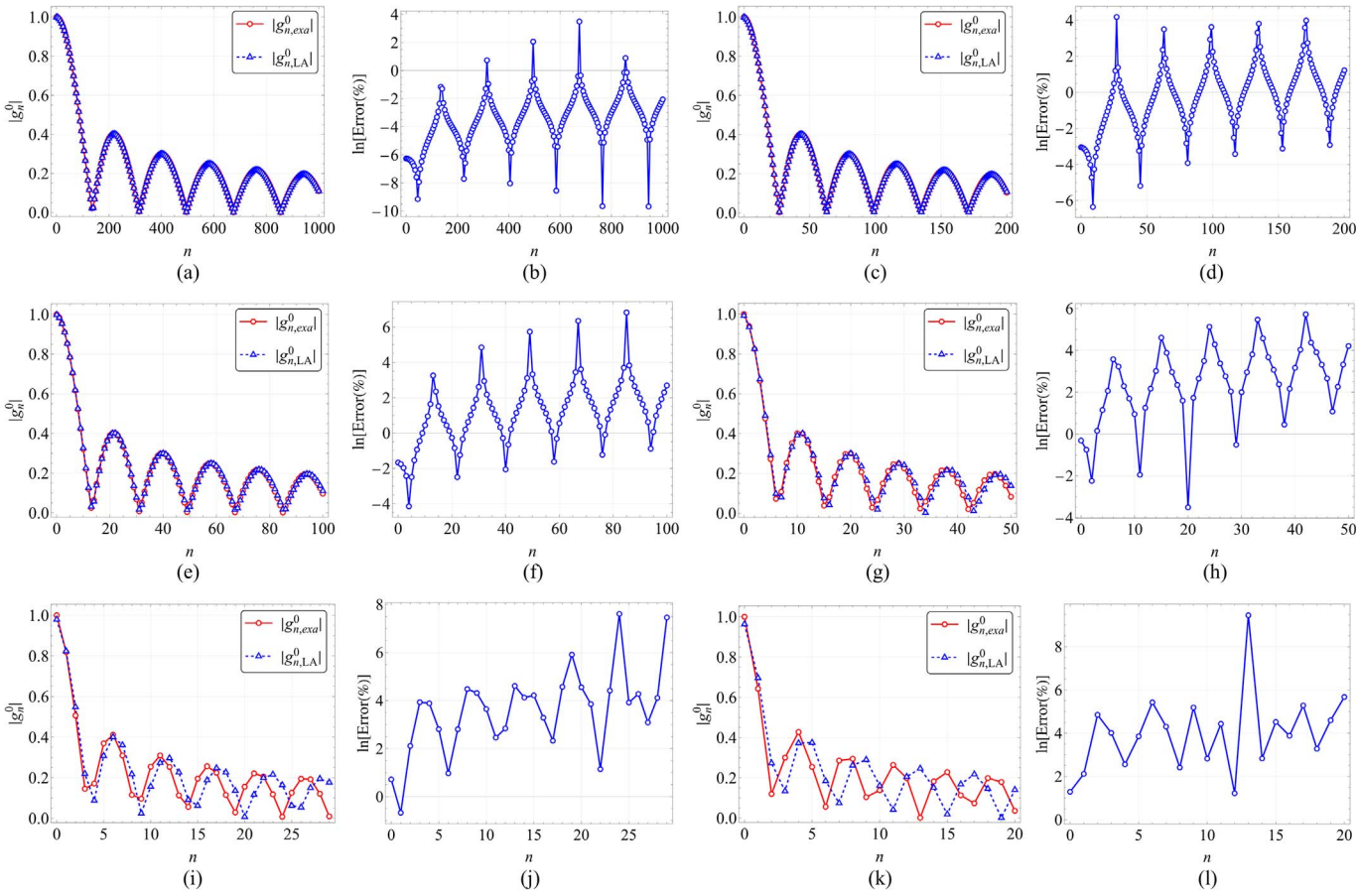

Figure 2. (a) Exact (red, solid, with circular marks) and LA (blue, dashed, with triangular marks) BSCs for an on-axis zero order Bessel beam as a function of n for $\alpha = 1°$. (b) The logarithmic percent error corresponding to (a). (c) and (d) $\alpha = 5°$; (e) and (f) $\alpha = 10°$; (g) and (h) $\alpha = 20°$; (i) and (j) $\alpha = 35°$; (k) and (l) $\alpha = 50°$. In all cases, $\lambda = 50$ μm.

are known, there is no need to actually go through the analytical process of finding the LA BSCs presented in previous sections. The disadvantage, of course, resides on the infinite summation, which not only can increase computational burden but also forces some truncation criterion to be imposed based on pre-specified tolerated error.

4 Simulations and results

In this section we illustrate the behavior of equations (19) and (21), and their simplified form for on-axis Bessel beams, equations (22) and (23), respectively, together with field reconstructions for both on-axis and off-axis beams with different axicon angles. To do so, in all simulations we have set $\lambda = 50$ μm. Algorithms have been developed based on the equations of the previous section using the commercial software *Wolfram Mathematica 12.1 Student Edition*. They are available upon reasonable request. Simulations were then run on a personal laptop [Intel(R) Core(TM) i7-3630QM CPU @ 2.40 GHz, 16.0 GB]. Arbitrary precision (infinite-precision arithmetic) has been chosen for the calculations.

The infinite sum in equation (1) is truncated in accordance with Wiscombe's convergence criterion [47], which is well-established in the field of optics and has also been recently introduced in acoustics and ultrasonics [24]. It states that there is a maximum n, say n_{max}, above which the partial waves will have negligible contribution to the total field. The value of n_{max} can be calculated in terms of the product kr, such that [47]:

$$n_{max} = \begin{cases} kr + 4(kr)^{1/3} + 1, & 0.02 \leq kr \leq 8 \\ kr + 4.05(kr)^{1/3} + 2, & 8 < kr < 4200 \\ kr + 4(kr)^{1/3} + 2, & 4200 \leq kr \leq 20,000. \end{cases} \quad (38)$$

As a first example, let us assume the simple on-axis configuration, for which $x_0 = y_0 = 0$. For this case, the only non-zero beam shape coefficients (BSCs) are g^0_n, as can be seen from equations (22) and (23).

Figure 2 shows exact and localized approximation (LA) BSCs $|g^0_n|$ for a zero-order Bessel beam ($v = 0$), for six different axicon angles ($\alpha = 1°$, $5°$, $10°$, $20°$, $35°$ and $50°$), along with the logarithmic percent error $\ln\left[100|(|g^0_{n,exa}| - |g^0_{n,LA}|)/|g^0_{n,exa}|\right]$. A 1% error therefore

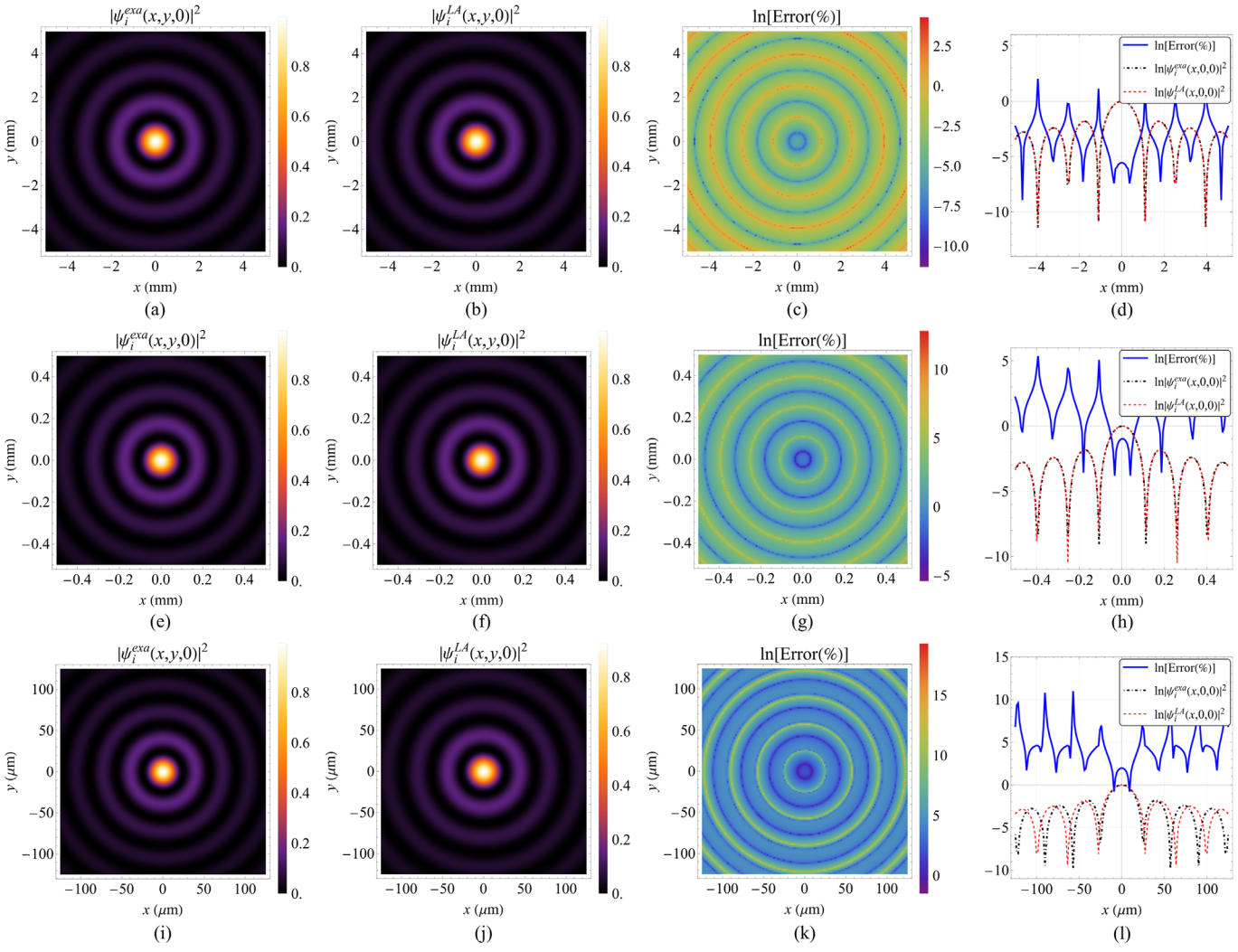

Figure 3. Exact and LA-remodeled field intensities $\left|\psi_i^{exa}(x,y,0)\right|^2$ and $\left|\psi_i^{LA}(x,y,0)\right|^2$, and logarithmic percent errors $\ln\left[100\left|\left(\left|\psi_i^{exa}(x,y,0)\right|^2-\left|\psi_i^{LA}(x,y,0)\right|^2\right)/\left|\psi_i^{exa}(x,y,0)\right|^2\right|\right]$ for the zero-order Bessel beams of Figure 2 with $\alpha=1°$, $10°$ and $50°$. (a)–(d) $\alpha=1°$. (e)–(h) $\alpha=10°$. (i)–(l) $\alpha=50°$. The corresponding BSCs are shown in Figure 2(a), (e) and (k), respectively.

corresponds to the horizontal line $\ln[\text{error}(\%)]=0$. Without loss of generality, we have set $z_0=0$.

Several important features are observed. First, the smaller the value of α, the better is the agreement between the exact and LA BSCs. However, notice that, for a fixed α, the logarithmic error slightly increases as n increases. The highest errors are seen for values of n coinciding with those points for which g_n^0 tends to zero. The most critical scenario is, of course, that of $\alpha=50°$. In this particular case, although both the exact and the LA BSCs show a similar oscillatory pattern (Fig. 2k), high errors are observed for all n (Fig. 2l), with the oscillations observed for the LA BSCs occurring for higher n when compared with those observed for the exact BSCs.

Such a delay clearly increases as α increases and reflects itself in the transverse locations of the bright annular disks of the Bessel beam. This is illustrated in Figure 3, where the exact and LA transverse field intensities, $\left|\psi_i^{exa}(x,y,0)\right|^2$ and $\left|\psi_i^{LA}(x,y,0)\right|^2$, together with the logarithmic error, are plotted for $\alpha=1°$ (Figs. 3a–3d), $10°$ (Figs. 3e–3h) and $50°$ (Figs. 3i–3l). It must be stressed that, even though subtle differences between the original (exact) and LA-remodeled beams can be noticed, the latter is a genuine acoustical beam on its own, that is, the remodeled beam is still an exact solution to the homogeneous scalar Helmholtz equation.

The effect of a non-zero topological charge can be appreciated in Figure 4 for $\alpha=50°$, which shows the exact and LA-remodeled field intensities for $v=0$, 3 and 7. One can clearly see that, as v increases, errors become higher at the positions of global maxima of $|\psi_i|$. This has important consequences on the application of localized schemes for predicting acoustic and ultrasonic pressure forces. Better results, at least at transverse positions close to the most intense bright annular disk, are expected for smaller values of v. In addition, for very small particles, only those partial waves with low values of n enter into the calculation of

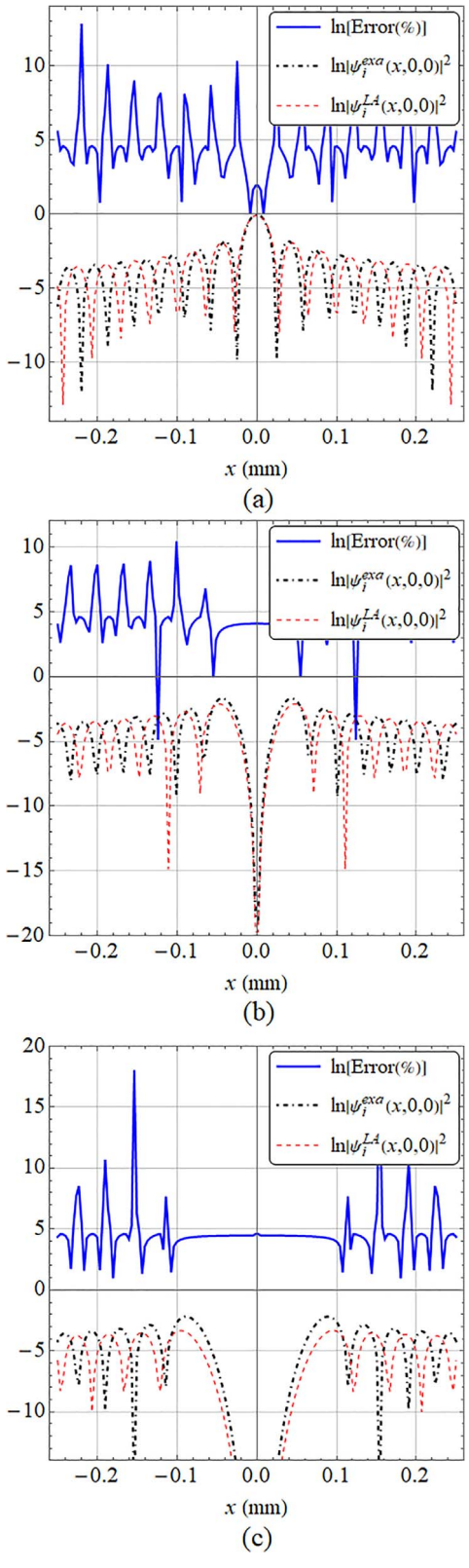

Figure 4. (a) Exact (black, dot-dashed) and LA-remodeled (red, dashed) field intensities $|\psi_i^{exa}(x,0,0)|^2$ and $|\psi_i^{LA}(x,0,0)|^2$ (in logarithmic scale), and logarithmic percent errors $\ln\left[100|(|\psi_i^{exa}(x,0,0)|^2 - |\psi_i^{LA}(x,0,0)|^2)/|\psi_i^{exa}(x,0,0)|^2|\right]$ for an on-axis Bessel beams with $\alpha = 50°$, for $v = 0$. (b) and (c) Same as (a), but now for $v = 3$ and 7, respectively.

acoustical forces, so that only the first few BSCs need to be taken into account. This means that, regardless of the value of α, the LA scheme might still produce good physical predictions. This is clearly seen for the zero-order Bessel beams of Figure 2 for all values of α, a feature also noticed in the optical domain [16].

For off-axis configuration, it can be seen from equations (19) and (21) that:

$$\frac{g^m_{n,LA}}{g^m_{n,exa}} = \left(\frac{1}{n+1/2}\right)^{|m|} \frac{(n+|m|)!}{(n-m)!} \frac{J_m\left[\left(n+\frac{1}{2}\right)\sin\alpha\right]}{P^m_n(\cos\alpha)}. \quad (39)$$

It is seen from equation (39) that the percent error $100|1 - |g^m_{n,LA}|/|g^m_{n,exa}||$ for a given n and m is actually independent of the relative lateral position or displacement (x_0, y_0) of the beam with respect to the origin O_P. Therefore, even though the number of BSCs demanded to reproduce $\psi_i(r,\theta,\phi)$ will increase for $\rho_0 \neq 0$ [this statement is readily confirmed from either equation (19) or (21) by setting $Z_0 \neq 0$], just like for on-axis beams, discrepancies between the exact and LA BSCs will only depend on n, m and α for off-axis Bessel beams. This means that the analysis of BSCs for the off-axis case resembles that previously performed for on-axis beams. This fact contrasts significantly with that observed for optical Bessel beams, for which the LA scheme could be highly dependent on x_0 and y_0 [16]. Finally, notice that the ratio $g^m_{n,LA}/g^m_{n,exa}$ is also independent of the beam order v.

As an example, Figure 5 shows how the ratio $g^m_{n,LA}/g^m_{n,exa}$ behaves as a function of n for a zero-order Bessel beam with $\alpha = 1°$ (Figs. 5a–5c), 10° (Figs. 5d–5f) and 30° (Figs. 5g–5i). Specific lateral displacements of $\rho_0 = 50\lambda$, 5λ and 4λ have been chosen with the sole purpose of having non-zero BSCs for $m \neq 0$, since equation (39) does not depend on ρ_0. The deleterious effect of an increasing axicon angle is readily seen. Such an effect becomes more pronounced at values of n corresponding to minima of $|g^m_{n,exa}|$.

An interesting feature of equation (39) is its independence with respect to the relative position (ρ_0, ϕ_0, z_0) of the Bessel beam. This means that, for a given axicon angle, the ratio between the LA and exact BSCs depends only on n and m. But it must be stressed that, since for fixed n and m the value of g^m_n changes as we move from an on-axis to an off-axis configuration, and also because g^m_n changes as $\rho_0 \neq 0$ changes, the reconstructed fields still depend on the relative position of the beam, as it should be.

An example of field reconstruction for an off-axis beam and from both exact and LA BSCs is illustrated in Figure 6 for $v = 0$ and $\alpha = 30°$, assuming $\rho_0 \equiv x_0 = 4\lambda = 200\ \mu$m. In acoustic scattering by spherical particles, force calculations assume that the particle is centered at O_P, that is, at $x = y = 0$. Since errors are high (Fig. 6c) the LA might fail to provide accurate force predictions for off-axis beams for such a high value of the axicon angle. It can be checked that smaller values of α improves the agreement between the original field and the one calculated through the LA.

As expected from the results for on-axis beams, notice that in Figure 6 there is a noticeable loss of symmetry in the Bessel pattern with respect to the optical axis of the

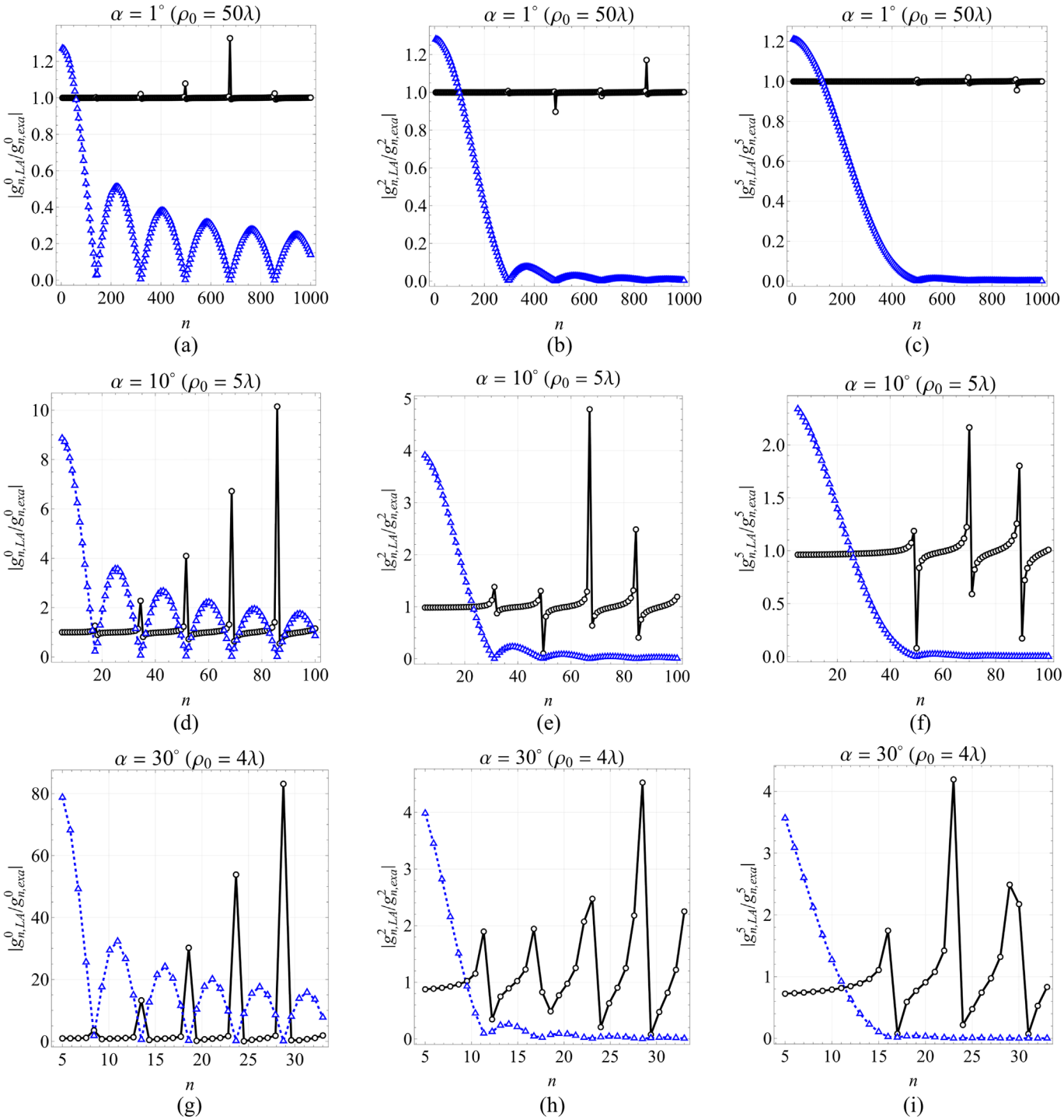

Figure 5. (a)–(c) Ratio $\left|g^m_{n,LA}/g^m_{n,exa}\right|$ (black solid lines, with circular marks) for a Bessel beam with $v = 0$ for $\alpha = 1°$ and $m = 0$, 2 and 5, respectively. (d)–(f) Same as before, now for $\alpha = 10°$. (g)–(i) Same as (a)–(c), now for $\alpha = 30°$. For reference purposes, the exact BSCs are also shown (blue dashed lines, with triangular marks), with multiplicative factors being introduced for better visualization. The choice of $\rho_0 \neq 0$ allows for non-zero BSCs for $m \neq 0$ but has not other implications in the comparison between the plots, since equation (39) does not depend on ρ_0 (had we chosen the same ρ_0, the results would remain unchanged). The beam is assumed to be displaced along the x axis, that is, $\phi_0 = 0$ or, equivalently, $\rho_0 = x_0$.

beam when using localization schemes (Fig. 6b). This comes from the fact that, as x increases, the number of BSCs demanded to calculate $\psi_i^{LA}(x, 0, 0)$ increases in accordance with the localization principle of van de Hulst (the same being valid for the field along y). But, as n increases, discrepancies between the exact and LA BSCs also increases, as revealed in Figure 2 for an on-axis Bessel beam.

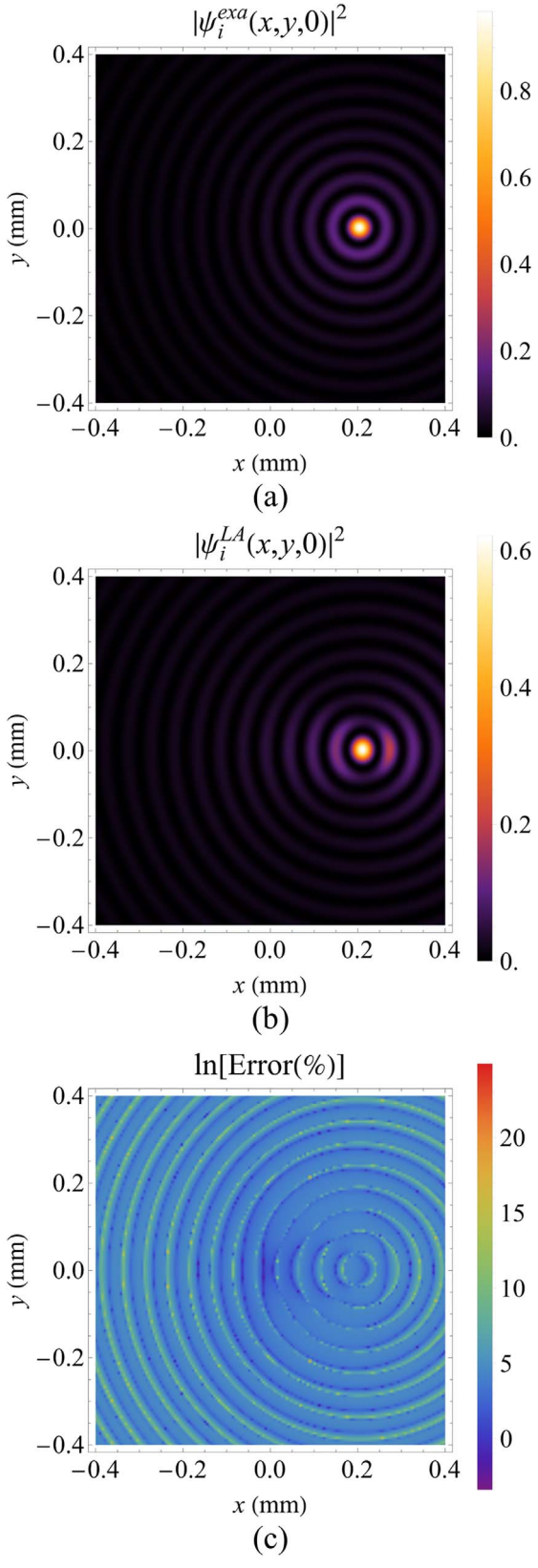

Figure 6. (a) Original transverse field intensity $|\psi_i(x, y, 0)|^2$ for an off axis zero-order Bessel beam with $\alpha = 30°$ and $\rho_0 = x_0 = 4\lambda$ ($y_0 = z_0 = 0$). (b) Same as (a), but now for the remodeled LA field using the BSCs given in equation (19). (c) Logarithmic percent error for the field intensities of (a) and (b).

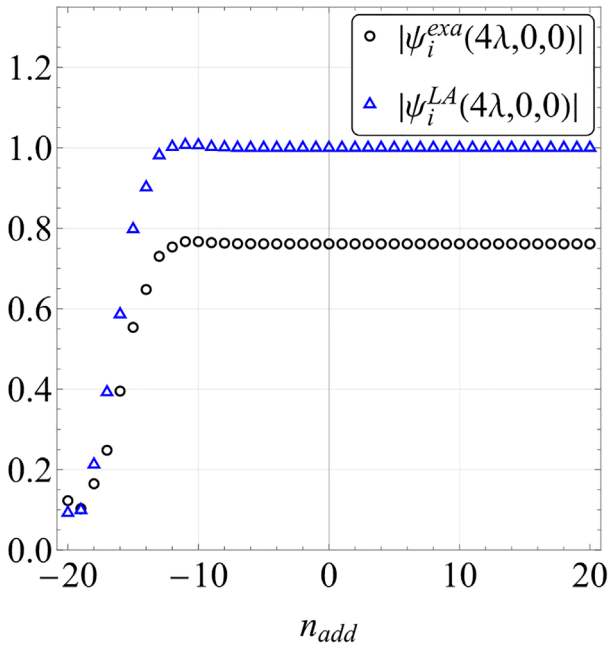

Figure 7. Verification of Wiscombe's criterion for the off-axis Bessel beam of Figure 6, at a fixed position $(x, y, z) = (4\lambda, y, z)$. Here, the value of n_{add} is added to that evaluated from Wiscombe's criterion [47], see equation (38) in order to truncate the sum in equation (1).

The choice of Wiscombe's criterion for truncating the sum in equation (1) has been qualitatively justified for Bessel beams by Ambrosio and Gouesbet in Ref. [24] (see Fig. 4 of this reference). In this work, the authors derived finite series expressions for the BSCs and compared them with those analytically extracted from quadratures. For field reconstruction using the LA method, a similar verification can be performed. Consider, for instance, adding or subtracting a value n_{add} from n_{max}, see equation (38). Figure 7 shows how $|\psi_i^{exa}(x = 4\lambda, 0, 0)|$ and $|\psi_i^{LA}(x = 4\lambda, 0, 0)|$ behave as n_{add} goes from -20 to 20, for the off-axis Bessel beam of Figure 6. As is clearly seen, as n_{add} approaches zero, that is, when truncation occurs at n_{max}, the calculated exact and LA field intensities have converged to their final values of 1 and 0.76129978, respectively, with excellent agreement.

Although ideally the LA method seeks to establish a complete identification $g_{n,LA}^m = g_{n,exa}^m$, such an identity is spoiled in view of equation (37). In fact, the LA BSCs are weighting sums of the exact coefficients with the same m. Because of equation (36), only those terms with $(p - |m|)$ even in the r.h.s. of equation (37) will contribute to the final value of $g_{n,LA}^m$, which means that, for even m, only the exact BSCs $g_{p,exa}^m$ with p even will contribute to the LA BSCs, while for m odd, only the exact BSCs with p odd will contribute to the LA BSCs. This is true not only for Bessel beams, but for any arbitrary-shaped beam.

As an example of application of equation (37), consider an on-axis Bessel beam ($z_0 = 0$) with $\alpha = 1°$ and $v = 0$. Table 1 shows $g_{n,LA}^0$ for specific values of n, as calculated from both equation (19) and equation (37), the latter being

Table 1. LA BSCs $g^{m}_{n,LA}$ as calculated from equations (19) and (37) using different truncation values for the sum over p. Here, $m = v = 0$, $x_0 = y_0 = z_0 = 0$ and $\alpha = 1°$.

n	Equation (19)	Equation (37) ($p = 20$)	Equation (37) ($p = 100$)	Equation (37) ($p = 400$)
1	0.999829	0.999829	0.999829	0.999829
5	0.997698	0.997698	0.997698	0.997698
10	0.991622	0.991620	0.991622	0.991622
25	0.951095	−0.140226	0.951095	0.951095
50	0.815034	−0.0812225	0.815034	0.815034
100	0.366731	0.0282588	0.285587	0.366731
200	−0.380019	0.00994502	0.010083	−0.380019

Table 2. Same as Table 1, now for $\alpha = 50°$.

n	Equation (19)	Equation (37) ($p = 20$)	Equation (37) ($p = 100$)	Equation (37) ($p = 400$)
1	0.696172	0.696172	0.696172	0.696172
5	−0.374691	−0.374691	−0.374691	−0.374691
10	0.161321	0.161320	0.161321	0.161321
25	0.179462	0.137049	0.179462	0.179462
50	0.125783	−0.0199318	0.125783	0.125783
100	0.0632092	0.00766147	0.059747	0.0632092
200	−0.0273322	0.00154104	0.00413776	−0.0273322

truncated at $p_{max} = 20$, 100, and 400. As p_{max} increases, there is greater agreement between the LA BSCs as computed from equations (19) and (37). This is also observed in Table 2 for $\alpha = 50°$, keeping all previous parameters unchanged.

5 Conclusions

In this work we have introduced the acoustical localized approximation for arbitrary-order Bessel beams. The beam shape coefficients have been compared with those computed from quadrature schemes and field remodeling has been shown for both on- and off-axis configurations.

In contrast with previous works which dealt with Gaussian beams, here we have justified the presence of pre-factors in the expressions for the localized approximation beam shape coefficients by having recourse to asymptotic behavior of associated Legendre functions of very large degrees. A rigorous justification of the localized approximation for arbitrary-shaped acoustic/ultrasonic beams is still open to investigation.

A variant of the localized approximation, which attempts at avoiding the decomposition of the original field into azimuthal modes, viz., the *integral* localized approximation, has also been presented. The beam shape coefficients for Bessel beams calculated in this manner are expectedly the same as those calculated from the original localization scheme. A general relationship between the localized and exact beam shape coefficients has been also provided, therefore eliminating the need to actually derive the former coefficients whenever the latter (exact) coefficients are available for any acoustic/ultrasonic beam.

The results shown in this paper reveals that the localized approximation can be used to describe acoustical and ultrasonic Bessel beams with (very) low axicon angles. For zero-order beams and small axicon angles, errors at the acoustical axis are usually small or negligible. However, as the order of the beam increases, the corresponding errors at the locations of maximum of the transverse field pattern (the most intense annular ring) increase as well, thus indicating that physical predictions involving, for instance, acoustic pressure force calculations and extracted from the localized beam shape coefficients might not be accurate enough in comparison with those computed from exact beam shape coefficients derived from quadrature schemes.

Obviously, the use of a localized approximation is superfluous when exact beam shape coefficients are available. However, this work has provided a path for a systematic and general justification of localized schemes for arbitrary-shaped beams. In the optical realm, justification has been given in terms of what is called the N-beam method [39]. Besides, it was also shown that the localized approximation cannot be rigorously justified for Bessel beams or, more in general, beams carrying a propagation factor of the form $\exp(-ik_z z)$ instead of $\exp(-ikz)$, e.g., Ref. [14]. We hope that the present work paves the way for equivalent deeper investigations in acoustics and ultrasonics.

Funding

This work was partially supported by the National Council for Scientific and Technological Development (CNPq) (406949/2021-2, 309201/2021-7) and by The São Paulo Research Foundation (FAPESP) (2021/06121-0).

Conflict of interest

The authors declare no conflict of interest.

Data availability statement

The data are available from the corresponding author on request.

References

1. G. Gouesbet, B. Maheu, G. Gréhan: Light scattering from a sphere arbitrarily located in a Gaussian beam, using a Bromwich formulation. Journal of the Optical Society of America A 5, 9 (1988) 1427–1443.
2. G. Gouesbet, G. Gréhan: Generalized Lorenz–Mie theories. 3rd edn., Springer, Switzerland, 2023.
3. P.C. Waterman: Symmetry, unitarity, and geometry in electromagnetic scattering. Physical Review D 3 (1971) 825–839.
4. M.I. Mishchenko, L.D. Travis, A.A. Lacis: Scattering, absorption, and emission of light by small particles, Cambridge University Press, Cambridge, UK, 2002.
5. M.I. Mishchenko: Electromagnetic scattering by particles and particle groups, an introduction, Cambridge University Press, Cambridge, UK, 2014.
6. G. Gouesbet, J.A. Lock, G. Gréhan: Generalized Lorenz–Mie theories and description of electromagnetic arbitrary shaped beams: localized approximations and localized beam models, a review. Journal of Quantitative Spectroscopy and Radiative Transfer 112, 1 (2011) 1–27.
7. J.A. Lock, G. Gouesbet: Rigorous justification of the localized approximation to the beam-shape coefficients in generalized Lorenz–Mie theory. I. On-axis beams. Journal of the Optical Society of America A 11, 9 (1994) 2503–2515.
8. G. Gouesbet, James A. Lock: Rigorous justification of the localized approximation to the beam-shape coefficients in generalized Lorenz–Mie theory. II. Off-axis beams. Journal of the Optical Society of America A 11, 9 (1994) 2516–2525.
9. K.F. Ren, G. Gouesbet, G. Gréhan: Integral localized approximation in generalized Lorenz–Mie theory. Applied Optics 37, 19 (1998) 4218–4225.
10. S. Li, J. Shi, X. Zhang: Study on acoustic radiation force of an elastic sphere in an off-axial Gaussian beam using localized approximation. The Journal of the Acoustical Society of America 151, 4 (2022) 2602–2612.
11. S. Li, X. Zhang: Three-dimensional acoustic radiation force of a eukaryotic cell arbitrarily positioned in a Gaussian beam. Nanotechnology and Precision Engineering 6, 1 (2023) 013005.
12. P.L. Marston: Acoustic beam scattering and excitation of sphere resonance: Bessel beam example. The Journal of the Acoustical Society of America 122, 1 (2007) 247–252.
13. P.L. Marston: Quasi-Gaussian Bessel-beam superposition: application to the scattering of focused waves by spheres. The Journal of the Acoustical Society of America 129, 4 (2011) 1773–1782.
14. G. Gouesbet: On the validity of localized approximations for Bessel beams: all N-Bessel beams are identically equal to zero. Journal of Quantitative Spectroscopy and Radiative Transfer 176 (2016) 82–86.
15. G. Gouesbet, J.A. Lock, L.A. Ambrosio, J.J. Wang: On the validity of localized approximation for an on-axis zeroth-order Bessel beam. Journal of Quantitative Spectroscopy and Radiative Transfer 195 (2017) 18–25. Laser-light and Interactions with Particles 2016.
16. L.A. Ambrosio, J. Wang, G. Gouesbet: On the validity of the integral localized approximation for Bessel beams and associated radiation pressure forces. Applied Optics 56, 19 (2017) 5377–5387.
17. A. Chafiq, L.A. Ambrosio, G. Gouesbet, A. Belafhal: On the validity of integral localized approximation for on-axis zeroth-order Mathieu beams. Journal of Quantitative Spectroscopy and Radiative Transfer 204 (2018) 27–34.
18. L.A. Ambrosio, L.F.M. Votto, G. Gouesbet, J. Wang: Assessing the validity of the localized approximation for discrete superpositions of Bessel beams. Journal of the Optical Society of America B 35, 11 (2018) 2690–2698.
19. N.L. Valdivia, L.F.M. Votto, G. Gouesbet, J. Wang, L.A. Ambrosio: Bessel-Gauss beams in the generalized Lorenz–Mie theory using three remodeling techniques. Journal of Quantitative Spectroscopy and Radiative Transfer 256 (2020) 107292.
20. G. Gouesbet, L.A. Ambrosio: On the validity of the use of a localized approximation for helical beams. I. Formal aspects. Journal of Quantitative Spectroscopy and Radiative Transfer 208 (2018) 12–18.
21. L.A. Ambrosio, G. Gouesbet: On the validity of the use of a localized approximation for helical beams. II. Numerical aspects. Journal of Quantitative Spectroscopy and Radiative Transfer 215 (2018) 41–50.
22. L.A. Ambrosio, G. Gouesbet: On localized approximations for Laguerre-Gauss beams focused by a lens. Journal of Quantitative Spectroscopy and Radiative Transfer 218 (2018) 100–114.
23. L.F.M. Votto, L.A. Ambrosio, G. Gouesbet: Evaluation of beam shape coefficients of paraxial Laguerre-Gauss beam freely propagating by using three remodeling methods. Journal of Quantitative Spectroscopy and Radiative Transfer 239 (2019) 106618.
24. L.A. Ambrosio, G. Gouesbet: Finite series approach for the calculation of beam shape coefficients in ultrasonic and other acoustic scattering. Journal of Sound and Vibration 585 (2024) 118461.
25. D. Baresch, J.-L. Thomas, R. Marchiano: Three-dimensional acoustic radiation force on an arbitrarily located elastic sphere. The Journal of the Acoustical Society of America 133, 1 (2013) 25–36.
26. D. Blackstock: Fundamentals of physical acoustics, John Wiley & Sons, New York, NY, 2000.
27. L. Robin: Fonctions sphériques de Legendre et fonctions sphéroidales, vol. 1, 2, 3, Gauthier-Villars, Paris, 1957.
28. T.S. Hart, M.F. Hamilton: Nonlinear effects in focused sound beams. The Journal of the Acoustical Society of America 84, 4 (1988) 1488–1496.
29. M.F. Hamilton, V.A. Khokhlova, O.V. Rudenko: Analytical method for describing the paraxial region of finite amplitude sound beams. The Journal of the Acoustical Society of America 101, 3 (1997) 1298–1308.
30. D.T. Blackstock, J.M. Cormack, M.F. Hamilton: Early history of nonlinear acoustics. Proceedings of Meetings on Acoustics 36, 1 (2020) 045007.
31. D. Blackstock: Fundamentals of physical acoustics, John Wiley & Sons, New York, USA, 2000.
32. A. Pierce: Acoustics: an introduction to its physical principles and applications. 3rd edn., Springer, Berlin, 2019.
33. G.B. Arfken, H.J. Weber: Mathematical methods for physicists, Harcourt/Academic Press, Burlington, MA, USA, 2001.
34. Z. Gong, P.L. Marston, Wei Li: T-matrix evaluation of three-dimensional acoustic radiation forces on nonspherical objects in Bessel beams with arbitrary order and location. Physical Review E 99 (2019) 063004.
35. H.C. van de Hulst: Light scattering by small particles. Dover books on physics, Dover Publications, New York, 1981.

36. F.G. Mitri, G.T. Silva: Off-axial acoustic scattering of a high-order Bessel vortex beam by a rigid sphere. Wave Motion 48, 5 (2011) 392–400.
37. F.G. Mitri: Acoustic scattering of a high-order Bessel beam by an elastic sphere. Annals of Physics 323, 11 (2008) 2840–2850.
38. T. Hasegawa: Comparison of two solutions for acoustic radiation pressure on a sphere. The Journal of the Acoustical Society of America 61, 6 (1977) 1445–1448.
39. G. Gouesbet: Validity of the localized approximation for arbitrary shaped beams in the generalized Lorenz–Mie theory for spheres. Journal of the Optical Society of America A 16, 7 (1999) 1641–1650.
40. P.S. Epstein, R.R. Carhart: The absorption of sound in suspensions and emulsions. I. Water fog in air. The Journal of the Acoustical Society of America 25, 3 (1953) 553–565.
41. P.A. Martin: On acoustic scattering of beams. Wave Motion 115 (2022) 103075.
42. L.A. Ambrosio, H.E. Hernández-Figueroa: Integral localized approximation description of ordinary Bessel beams and application to optical trapping forces. Biomedical Optics Express 2, 7 (2011) 1893–1906.
43. J. Durnin: Exact solutions for nondiffracting beams. I. The scalar theory. Journal of the Optical Society of America A 4, 4 (1987) 651–654.
44. J. Durnin, J. Miceli Jr, J.H. Eberly: Diffraction-free beams. Physical Review Letters 58, 15 (1987) 1499–1501. cited By 2754.
45. G.N. Watson: A treatise on the theory of Bessel functions, Cambridge University Press, Cambridge, UK, 1944.
46. R. Li, K.F. Ren, X. Han, Z. Wu, L. Guo, S. Gong: Analysis of radiation pressure force exerted on a biological cell induced by high-order Bessel beams using Debye series. Journal of Quantitative Spectroscopy and Radiative Transfer 126 (2013) 69–77. Lasers and interactions with particles 2012.
47. W.J. Wiscombe: Improved Mie scattering algorithms. Applied Optics 19, 9 (1980) 1505–1509.

Cite this article as: Ambrosio LA & Gouesbet G. 2024. A localized approximation approach for the calculation of beam shape coefficients of acoustic and ultrasonic Bessel beams. Acta Acustica, **8**, 26.